Long bunch trains measured using a prototype cavity beam position monitor for the Compact Linear Collider

F. J. Cullinan,[1,*] S. T. Boogert,[1] W. Farabolini,[2] T. Lefevre,[2] A. Lunin,[3] A. Lyapin,[1] L. Søby,[2] J. Towler,[1,2] and M. Wendt[2]

[1]*John Adams Institute at Royal Holloway, University of London, Surrey TW20 0EX, United Kingdom*
[2]*CERN, Geneva, 1217 Meyrin, Switzerland*
[3]*Fermilab, Batavia, Illinois 60510, USA*

(Received 29 January 2015; revised manuscript received 4 October 2015; published 19 November 2015)

The Compact Linear Collider (CLIC) requires beam position monitors (BPMs) with 50 nm spatial resolution for alignment of the beam line elements in the main linac and beam delivery system. Furthermore, the BPMs must be able to make multiple independent measurements within a single 156 ns long bunch train. A prototype cavity BPM for CLIC has been manufactured and tested on the probe beam line at the 3rd CLIC Test Facility (CTF3) at CERN. The transverse beam position is determined from the electromagnetic resonant modes excited by the beam in the two cavities of the pickup, the position cavity and the reference cavity. The mode that is measured in each cavity resonates at 15 GHz and has a loaded quality factor that is below 200. Analytical expressions for the amplitude, phase and total energy of signals from long trains of bunches have been derived and the main conclusions are discussed. The results of the beam tests are presented. The variable gain of the receiver electronics has been characterized using beam excited signals and the form of the signals for different beam pulse lengths with the 2/3 ns bunch spacing has been observed. The sensitivity of the reference cavity signal to charge and the horizontal position signal to beam offset have been measured and are compared with theoretical predictions based on laboratory measurements of the BPM pickup and the form of the resonant cavity modes as determined by numerical simulation. Finally, the BPM was calibrated so that the beam position jitter at the BPM location could be measured. It is expected that the beam jitter scales linearly with the beam size and so the results are compared to predicted values for the latter.

DOI: 10.1103/PhysRevSTAB.18.112802 PACS numbers: 29.20.Ej

I. INTRODUCTION

The Compact Linear Collider (CLIC) is a proposed electron-positron collider with a maximum center of mass energy of 3 TeV. Its distinguishing feature is the drive beam, a high current, low energy electron beam that transfers energy, in the form of radio frequency (rf) power, to the 12 GHz normal conducting accelerating structures throughout the length of the main beam linac [1]. The main parameters of the CLIC main beams are given in Table I.

In order to achieve the target luminosity, each main beam must be transported through the main linac and beam delivery system without compromising the beam size at the interaction point. For this reason, the accelerator elements in these sections must be aligned more precisely than is possible with surveying methods alone. A beam based alignment is therefore employed. This is based on a dispersion-free steering algorithm which minimizes the difference in trajectory between a bunch train at the nominal energy and a bunch train at a lower energy [2]. For this, the beam position monitors (BPMs) must measure the transverse position of the beam along its trajectory with a resolution of 50 nm. As well as using multiple beam pulses for the dispersion free steering, the possibility of using a single bunch train with an energy chirp along it must be accommodated. Each BPM must therefore be able to make multiple independent position measurements within a single 156 ns long bunch train [3]. The highest demands on the BPM system are in the beam delivery system where, close to the interaction point, a position resolution of 3 nm is required [1]. In order to achieve these resolutions, the use of cavity beam position monitors is proposed since they have been shown to routinely reach resolutions in the order of 10 nm [4].

A. Cavity beam position monitor principle

A cavity BPM pickup consists of at least one cavity with the beam pipe passing through the middle. When a charged particle bunch traverses a cavity, it excites multiple resonant electromagnetic modes. These modes are predominantly transverse magnetic (TM) which means that, aside from the effects of the beam pipe and the signal extraction,

*Francis.Cullinan.2010@live.rhul.ac.uk

TABLE I. Parameters of the main beams of the Compact Linear Collider [1].

Parameter	Value
Bunching frequency	2 GHz
Train length	156 ns
Bunch charge	0.6 nC
Maximum center of mass energy	3 TeV
Beam size at interaction point x/y	45/1 nm
Target luminosity	2×10^{34} cm^{-2} s^{-1}
Beam delivery system length	2.75 km
Main linac length	21 km

they have no longitudinal magnetic field component B_z [5]. The different TM modes are distinguished by the number of oscillations in the electromagnetic field amplitudes along the coordinate axes, denoted by the three subscript indices n, m and l, i.e., $\mathrm{TM}_{\mathrm{nml}}$. In the case of cylindrical cavities, the indices refer to the three cylindrical coordinates ϕ, ρ and z respectively and the first dipole mode TM_{110} and the first monopole mode TM_{010} are measured to obtain the beam position. Each mode oscillates in time with a characteristic resonant angular frequency ω. The strength of the coupling between the relativistic beam and a mode is well parametrized by the mode's normalized shunt impedance R/Q given by

$$\frac{R}{Q} = \frac{1}{\omega U}\left|\int_{-\infty}^{+\infty} E_z(x,y,z)e^{-i\frac{\omega z}{c}}dz\right|^2, \tag{1}$$

where E_z is the longitudinal component of the electric field and U is the electromagnetic energy stored in the mode. For small offsets, the R/Q of the first dipole mode is proportional to the square of the position offset from the cavity center while the R/Q of a monopole mode is position independent.

Over each oscillation period, a fraction of the energy stored in a mode, given by the mode's external quality factor Q_{ext}, is coupled out of the cavity. Immediately after excitation, the resulting output power P_{out} is given by

$$P_{\mathrm{out}} = \frac{\omega^2}{4Q_{\mathrm{ext}}}\left(\frac{R}{Q}\right)q^2 e^{-\omega^2\sigma_t^2}, \tag{2}$$

where q is the bunch charge and the normalized shunt impedance R/Q is at the transverse position of the beam. The exponential factor accounts for the length of the charged particle bunch in time σ_t assuming a Gaussian distribution in time [6]. Under the approximation that the mode output power is constant over one complete oscillation period, the peak output voltage V_{out} is given by

$$V_{\mathrm{out}} = \sqrt{2P_{\mathrm{out}}Z_0}, \tag{3}$$

where Z_0 is the load impedance. Once the modes are excited, the output voltage V oscillates in time t at the mode resonant frequency and decays exponentially as energy is extracted:

$$V(t) = V_{\mathrm{out}}e^{-\frac{t}{\tau}}\sin(\omega t), \tag{4}$$

where the decay time τ is given by

$$\tau = \frac{2Q_L}{\omega}. \tag{5}$$

Q_L is the loaded quality factor which includes energy losses in the cavity walls as well as the energy coupled out.

The output voltage from a dipole mode excited in a cavity by the beam can be measured, the charge dependence can be removed using a monopole mode and the beam position can be determined. There are further contributions to the measured dipole mode amplitude from the beam trajectory angle and the bunch tilt. These add in quadrature phase to the contribution from the beam position offset. The monopole mode signal can be used to provide a reference phase that is fixed with respect to the beam arrival time and the phase of the dipole mode signal relative to the monopole mode signal can be used to remove the beam trajectory angle and bunch tilt contributions. For this purpose, the dipole and monopole modes should have the same resonant frequency and so two separate cavities are commonly used, one for each mode. The cavity in which the dipole mode is measured is referred to as the position cavity while the monopole mode cavity is referred to as the reference cavity [6].

B. Signals from multiple bunches

An output signal excited by a single bunch in a cavity BPM pickup is the decaying sinusoid of Eq. (4). When multiple bunches pass through a pickup cavity with a time separation that is not significantly longer than the decay time of the cavity mode being measured, the signals from the different bunches overlap and are summed with some time offset between them. If the signal from each individual bunch has the same initial amplitude A_0 and phase ϕ_0, upon the arrival of the Nth bunch, the total signal output voltage $V_{\mathrm{out}}(N)$ is given, in complex form, by

$$V_{\mathrm{out}}(N) = \sum_{n=0}^{N-1} A_0 e^{-\frac{nt_b}{\tau}}e^{i(n\omega t_b+\phi_0)}, \tag{6}$$

where t_b is the time between consecutive bunches and t_b, ω, τ and ϕ_0 are all real numbers. Equation (6) is the sum of a geometric series and so it can be expressed without the summation [7]. Because of the way the signals are processed, outlined in Sec. I E, it is convenient to separate the signal amplitude $A(N)$ and phase $\phi(N)$, which respectively correspond to the modulus and argument of the complex result. This gives

$$\frac{A(N)}{A_0} = \sqrt{\frac{1 - 2C(N) + e^{-\frac{2Nt_b}{\tau}}}{1 - 2C(1) + e^{-\frac{2t_b}{\tau}}}} \tag{7}$$

and

$$\phi(N) - \phi_0 = \tan^{-1}\left(\frac{S(1) + e^{-\frac{2t_b}{\tau}}S(N-1) - S(N)}{1 - C(1) + e^{-\frac{2t_b}{\tau}}C(N-1) - C(N)}\right), \tag{8}$$

where

$$S(m) = e^{-\frac{mt_b}{\tau}}\sin(m\omega t_b) \quad \text{and} \tag{9}$$

$$C(m) = e^{-\frac{mt_b}{\tau}}\cos(m\omega t_b) \tag{10}$$

are defined for compactness.

Between the arrival of each bunch, the signal will evolve in the same way as the single bunch signal so that

$$V(N,t) = A(N)e^{-\frac{t}{\tau}}e^{i[\omega t + \phi(N)]}. \tag{11}$$

The geometric ratio in Eq. (6), $\exp(-t_b/\tau)\exp(i\omega t_b)$, is of modulus less than one and so the summation converges. The amplitude and phase at convergence can be found by evaluating Eqs. (7) and (8) in the limit of an infinite number of bunches N. The convergence of the phase means that the multiple bunch signal becomes periodic at the bunching frequency. Figure 1 shows Eqs. (7) and (8) evaluated at different cavity mode resonant frequencies for $t_b = 2/3$ ns and $\tau = 10$ ns. This decay time is significantly longer than the decay times of the signal modes in the CLIC prototype (see Sec. I C). It was chosen for illustrative purposes so that the convergence in Fig. 1 is not too fast. It can be seen that where the cavity mode resonant frequency is a harmonic of the bunching frequency $1/t_b$, the increase in amplitude with the number of bunches is simply given by

$$\frac{A(N)}{A_0} = \frac{1 - e^{-\frac{Nt_b}{\tau}}}{1 - e^{-\frac{t_b}{\tau}}} \tag{12}$$

and throughout the signal, the phase is the same at the arrival of each bunch. When this resonance condition is not met, there is some beating between the cavity mode resonant frequency and the bunching harmonic before the convergence.

Figure 2 shows the convergence limits in amplitude and phase for different decay times. It shows that where the cavity mode resonant frequency is a harmonic of the bunching frequency, there is a peak in the amplitude limit and the phase advance limit is 0. As the decay time is shortened, the signal decays more between the arrival of each bunch and the amplitude limit varies less with the mode resonant frequency.

The total signal energy can be determined by integrating the signal output power over time t. The output power is proportional to the square of the voltage amplitude. It decays exponentially between consecutive bunches with half the cavity mode decay time τ and decays continually after the arrival of the last bunch. Therefore, the total output signal energy after N bunches is given by

$$E(N) = \sum_{n=0}^{N-1}\left[\left(\frac{A(n)}{A_0}\right)^2\int_0^{t_b} P_{\text{out}}e^{-\frac{2t}{\tau}}dt\right] + \left(\frac{A(N)}{A_0}\right)^2\int_0^{\infty} P_{\text{out}}e^{-\frac{2t}{\tau}}dt, \tag{13}$$

where $P_{\text{out}} = V_{\text{out}}^2(1)/(2Z_0)$ is the output power from a single bunch signal. In the case where the cavity mode

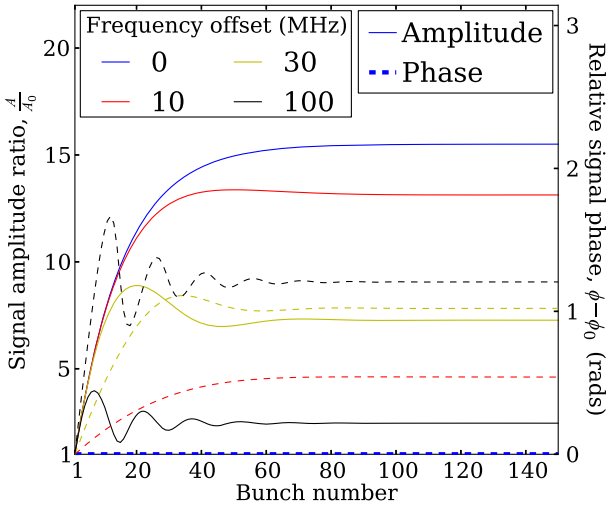

FIG. 1. Signal rise in amplitude and phase against the number of bunches as predicted by Eqs. (7) and (8).

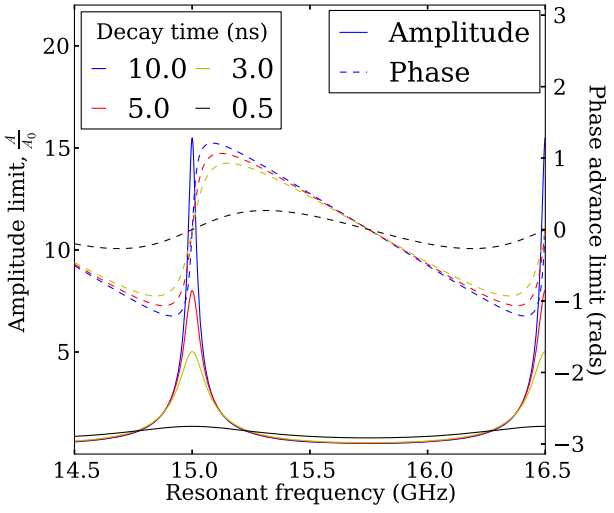

FIG. 2. Convergence limits in amplitude and phase of the multiple bunch signal as the number of bunches tends to infinity.

resonant frequency is an exact harmonic of the bunching frequency, Eq. (12) can be used for $A(n)/A_0$. Evaluating the integrals and the summation then gives

$$E(N) = \left(\left[N - 2\left(\frac{1-e^{-\frac{Nt_b}{\tau}}}{1-e^{-\frac{t_b}{\tau}}}\right) + \left(\frac{1-e^{-\frac{2Nt_b}{\tau}}}{1-e^{-\frac{2t_b}{\tau}}}\right)\right] \times \frac{1-e^{-\frac{2t_b}{\tau}}}{(1-e^{-\frac{t_b}{\tau}})^2} + \left[\frac{1-e^{-\frac{Nt_b}{\tau}}}{1-e^{-\frac{t_b}{\tau}}}\right]^2\right)\frac{P_{\text{out}}\tau}{2}. \quad (14)$$

For completeness, Eq. (13) is also evaluated for the more general case where the cavity mode resonant frequency is not a harmonic of the bunching frequency. The resulting expression is

$$E(N) = \left(\left[\frac{1-e^{-\frac{2t_b}{\tau}}}{1-2C(1)+e^{-\frac{2t_b}{\tau}}}\right] \times \left[N + \left(\frac{1-e^{-\frac{2Nt_b}{\tau}}}{1-e^{-\frac{2t_b}{\tau}}}\right) - 2\left(\frac{1+e^{-\frac{2t_b}{\tau}}C(N-1) - 2C(N) - 2C(1)}{1-2C(1)+e^{-\frac{2t_b}{\tau}}}\right)\right] + \left[\frac{1-2C(N)+e^{-\frac{2Nt_b}{\tau}}}{1-2C(1)+e^{-\frac{2t_b}{\tau}}}\right]\right)\frac{P_{\text{out}}\tau}{2}. \quad (15)$$

C. Prototype cavity BPM for CLIC

A prototype cavity BPM pickup for CLIC was designed at Fermilab [8]. The pickup has been manufactured and was installed on the probe beam line of the 3rd CLIC test facility (CTF3) at CERN for beam tests during the three month running period during the Spring of 2013. An image of the manufactured pickup is shown in Fig. 3. It includes two cylindrical cavities and a beam pipe with the same 8 mm diameter as the beam pipe in the CLIC main linac.

The vacuum geometry of the prototype pickup is shown on the right of Fig. 3. The position cavity is designed to selectively extract energy from the pair of orthogonal dipole mode polarizations magnetically coupled to the four rectangular waveguides. Each polarization is sensitive to the beam offset along a different Cartesian axis and so

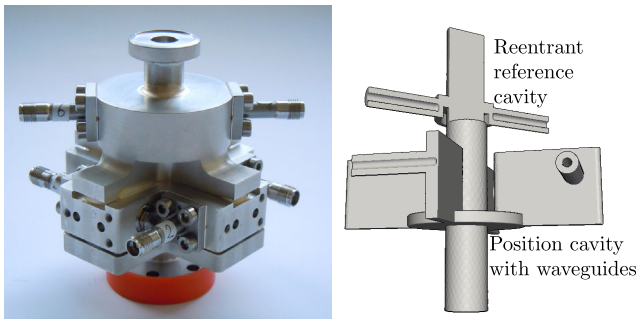

FIG. 3. Image of the cavity BPM pickup assembly (left) with the position cavity at the bottom and the reentrant reference cavity at the top and the vacuum geometry (right).

independent measurements of the vertical and horizontal beam position can be made. Monopole modes are rejected since their magnetic fields are perpendicular to that of the dominant waveguide mode and the lowest monopole mode TM_{010} is further rejected because its resonant frequency is below the waveguide cutoff frequency. The resonant frequencies f_0 of the first dipole mode in the position cavity and the first monopole mode in the reentrant reference cavity are both 15 GHz. This is a harmonic of the 1.5 GHz bunching frequency of the CTF3 probe beam line so that these modes constructively interfere when excited by multiple bunches while other nonsignal modes interfere destructively. The pickup is made from stainless steel which has a low electrical conductivity so that the resonant modes have low quality factors and the signal from any one bunch decays fast enough for multiple independent measurements to be made within the duration of a single CLIC bunch train [8].

The resonant modes of the BPM pickup were measured in the laboratory using a network analyzer. The important characteristics after brazing of the assembly are summarized in Table II. where the decay times have been calculated using Eq. (5). The measured external quality factor of the reference cavity monopole mode differs considerably from its design value because the geometry had to be modified to correct the resonant frequency. The difference in the loaded quality factor of the position cavity compared to the prediction is most probably due to surface roughness and nonideal electrical contacts of the brazed mechanical assembly [9].

The sensitivity of the pickup was predicted from the measured external quality factors and the normalized shunt impedances, determined for the modes of interest using the 3D electromagnetic simulation codes ACE3P [10] and GdfidL [11]. The R/Q of the position cavity dipole mode was evaluated at a 1 mm position offset along its axis of polarization. A summary of the sensitivity calculation using Eqs. (2) and (3) is shown in Table III. An extra reduction factor of $1/\sqrt{2}$ has been included since only one of the two output ports that can be used to measure each mode is used while the other is terminated in a matched load. The exponential factor has been applied with the CALIFES root mean square (rms) bunch length $\sigma_t = 4.25$ ps (see Sec. I D).

TABLE II. Parameters of the resonant cavity modes in the cavity BPM pickup as measured using a network analyzer in comparison to those predicted from simulation [9].

Parameter	Position cavity TM_{110}		Reference cavity TM_{010}	
	Design	Measured	Design	Measured
f_0 (GHz)	15.0	15.012	15.0	14.997
Q_L	261	198	120	130
Q_{ext}	630	617	275	203
τ (ns)	5.5	4.2	2.5	2.8

TABLE III. Calculation of the predicted sensitivities of the reference cavity to charge and the position cavity to beam charge and position.

Cavity	Code	(R/Q) (Ω)	Q_{ext}	Sensitivity (V nC^{-1})
Position	ACE3P	3.27	617	20.6 mm^{-1}
	GdfidL	3.26		20.6 mm^{-1}
Reference	ACE3P	50.7	203	142
	GdfidL	50.3		141

There is good agreement between the two simulation codes: to three significant figures for the position cavity dipole mode and two significant figures for the reference cavity monopole mode. The R/Q determined using GdfidL is used for the reference cavity sensitivity quoted later in comparison with the measured result.

D. CALIFES installation

The 3rd CLIC Test Facility is the latest experiment built to demonstrate the feasibility of the CLIC two beam acceleration scheme. It includes a drive beam that is designed to reach a maximum current of 32 A. This can be used to test accelerating structures that are installed in the probe beam line CALIFES (Concept d'Accélérateur Linéar pour Faisceau d'Électron Sonde). A diagram of CALIFES is shown in Fig. 4 and the important beam parameters are listed in Table IV. The photocathode injector and rf gun are able to provide bunches of up to 0.6 nC in charge. This can be varied by changing the incident power of the photoinjector laser on the cathode and can be measured using the integrating current transformer (ICT) after the rf gun. The beam pulse length, and thus, the number of bunches in the train, can also be adjusted by changing the duration of the laser pulse on the cathode. Bunch trains of any length between 1 and 226 bunches can be generated. The bunch length is defined by the 10 ps full width at half maximum laser pulse length [12] and has been measured directly [13]. Three 3 GHz accelerating structures accelerate the generated beam to around 200 MeV. The beam energy can be measured precisely using the spectrometer bending magnet before the final beam dump [14]. The CALIFES beam line is instrumented along its length with two types of beam position monitor, one type based on a reentrant cavity [15] and one type with an inductive pickup [16]. The beam line also includes six beam profile monitors, each with a scintillation screen of yttrium aluminium garnet (YAG) and/or an optical transition radiation screen made of silicon [17].

The prototype cavity BPM pickup is installed at the end of the probe beam line after the final spectrometer magnet as indicated in Fig. 4. At this location, its small 8 mm aperture does not interfere with the testing of accelerating structures in the two beam test stand. The beam can also be diverted using the upstream spectrometer bending magnet so that the BPM electronics are protected from high power beam configurations that may be used during normal running. The pair of two-axis dipole corrector magnets upstream also allows the beam position in the pickup to be varied both horizontally and vertically.

Receiver electronics are installed close to the pickup that down-convert the 15 GHz output signals to an intermediate frequency (IF) of around 200 MHz in a single stage. A single electronics channel is shown in Fig. 5. The gain of the electronics can be varied between −10 dB and +5 dB using a remotely controlled variable attenuator (HMC941LP4E from Hittite [18]) at the front end and the bandwidth is limited to about 200 MHz for the purposes of mode selection, image frequency rejection and antialiasing. More details of the analogue processing are given in [9] and [19].

Three identical electronics channels are installed close to the pickup. The gain, output power for 1 dB compression (OP1dB) and 3 dB bandwidth of each channel, as measured in the laboratory are listed in Table V. 20 dB of fixed attenuation is added between the output port of the reference cavity and the input of its electronics channel while 6 dB is added before the input of both the horizontal (X) and vertical (Y) position cavity channels. Because the excitation of pickup by the beam is not perfectly reproducible in the lab, some features of the electronics were also measured during the beam tests.

The electronics output is transferred to a four channel digitizer with 10 bit resolution and a 2 GS s^{-1} sampling rate (DC282 from Acqiris [20]), which is located in the CTF3 klystron gallery. Figure 6 shows two examples of digitized signals at 200 MHz from two different beam pulse lengths. The differences between short and long

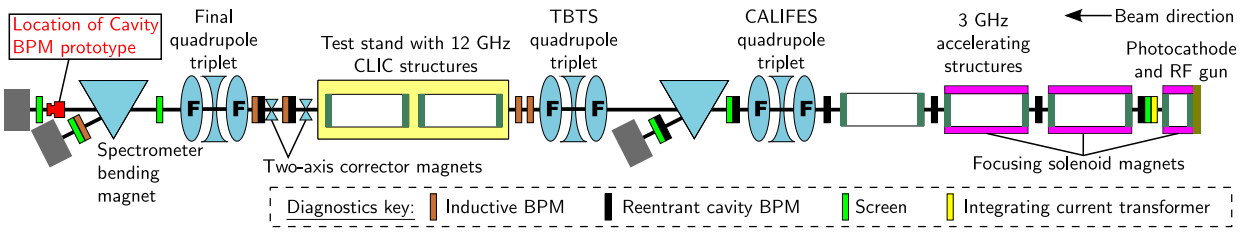

FIG. 4. Diagram of the CALIFES beam line showing the location of all major diagnostics, the prototype cavity BPM installation and the two dipole corrector magnets that were used to measure the position sensitivity of the pickup.

TABLE IV. Nominal beam parameters of CALIFES [14].

Parameter	Value
Energy	200 MeV
Repetition rate	1.6 Hz
Bunch charge	0.6 nC
rms bunch length	4.25 ps
Number of bunches	1–226

pulses were measured and are discussed in detail in Sec. II B. The digitizer is connected to and controlled over the CERN Open Analogue Signal Information System (OASIS), which features a graphical signal viewer [21]. OASIS is based on the front end software architecture that provides a hardware independent interface for acquiring signals [22]. In addition to the down-converter electronics, a rectifying diode is installed on one of the reference cavity output ports for preliminary sensitivity measurements [19].

E. Digital signal processing

For the purposes of beam position measurements, as discussed in Sec. I A, the signal amplitude and phase must be known. These are extracted from the signals digitized at the 200 MHz IF by digital down-conversion (DDC). The digitized signal is multiplied by a digital complex local oscillator (LO), also at the IF. This results in a signal component at baseband and an additional component at twice the IF. The high frequency component is removed using a finite impulse response Gaussian filter with a 67 MHz high frequency cutoff. If the LO and filter are normalized correctly, the signal at baseband $V_{\mathrm{DDC}}(t)$ from a single bunch excitation is approximately given by

$$V_{\mathrm{DDC}}(t) = GV_{\mathrm{out}}e^{-\frac{t}{\tau}}e^{i\phi}, \tag{16}$$

where G is the voltage gain of the analogue signal processing and transport and ϕ is the phase of the signal relative to the digital LO. The frequency of the digital LO must be determined precisely using a sample of digitized signals and then kept constant. It is found by minimizing the change in phase ϕ over time after down-conversion and filtering of the signal (as in [4]). Equation (16) is only evaluated at the times of the digital samples and so is discrete. The amplitude and phase of the baseband signal are sampled at a single point [4].

The sampled amplitude A and phase ϕ of the position and reference cavity signals are used to define in-phase I and quadrature-phase Q signal components as

$$I + iQ = \frac{A_p}{A_r}e^{i(\phi_p - \phi_r)}, \tag{17}$$

where the subscripts p and r denote the position and reference signals respectively. In order to make position measurements using the cavity BPM, two calibration constants must be determined. The first is the IQ rotation angle θ_{IQ}, by which the I and Q signal components are rotated to one component that corresponds to beam position and another that corresponds to beam trajectory angle and bunch tilt [4]. The second constant is the position scale factor s that converts the position component to physical units, millimeters in the case of the CTF3 prototype. The application of the calibration constants to determine the beam position P in physical units can be written as

$$P = s\{\mathrm{Re}([I + iQ]e^{i\theta_{IQ}})\}. \tag{18}$$

A beam based calibration is typically used to determine the two calibration constants. The position of the beam in the cavity BPM pickup is scanned across a known range.

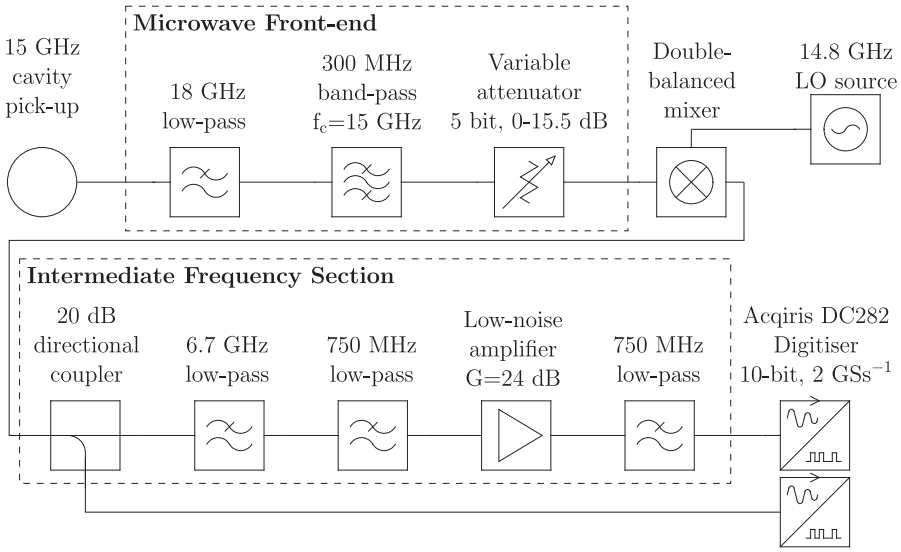

FIG. 5. Design of a single digital down-converter channel used for the beam measurements.

TABLE V. Parameters of the three channels of down-converter electronics as measured in the laboratory including the output power for 1 dB compression (OP1dB).

Parameter	X	Y	Reference
Gain (dB)	5.0	5.19	4.13
OP1dB (dBm)	13	13	13
Bandwidth (MHz)	216	204	205

It is assumed that the largest changes in the signal amplitude and phase during the scan are due to changes in the beam position only. This allows the IQ rotation angle θ_{IQ} and the position scale factor s to be determined. A calibration procedure for the CLIC cavity BPM prototype is described in Sec. III.

The main goal of the beam tests was to measure the pickup sensitivity. In order to compare the measured sensitivities with the predictions, the signal energy was simply measured by integrating the digitized waveforms using the rectangle rule as

$$E = \frac{\Delta t}{G^2 Z_0} \sum_{j=0}^{N} V_j^2, \tag{19}$$

where Z_0 is the load impedance of 50 Ω, Δt is the time between digitizer samples, N is the total number of digitizer samples and V_j is the signal voltage measured at sample j [6]. The measured signal energy can be compared with the result of Eq. (14), in which the signal decay time is calculated from the loaded quality factor of the resonant mode as measured in the laboratory and listed in Table II.

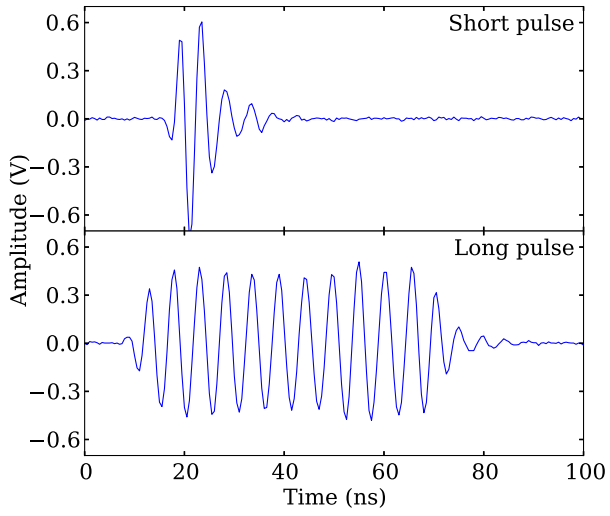

FIG. 6. Example digitized signals from the horizontal position channel of the cavity BPM excited by a short beam pulse and a long beam pulse.

II. BEAM MEASUREMENTS

At the start of the three months of beam tests, the hardware was debugged and the electronics were measured using the beam excited signals. In particular, the variable gain of the electronics was tested. Signals were also recorded for different beam pulse lengths in order to investigate the pickup response to the unique CALIFES bunch structure and to compare it with the analytical predictions outlined in Sec. I B. Single bunch operation with a stable bunch charge was not possible but it could be approximated using beam pulse lengths of 2 ns, which corresponds to about 2–3 bunches. The nominal bunch charge of 0.6 nC could not be achieved due to degradation of the photocathode. Typically, 0.05 nC bunches were used for both short and long beam pulses. Measurements of different pulse lengths with the same bunch charge were possible thanks to the variable gain of the electronics. Reliable and reproducible performance from the variable attenuator was therefore crucial for converting between results for the different pulse lengths.

The sensitivity of the reference cavity signal to charge was measured by varying the power of the photoinjector laser on the cathode and comparing the reference cavity signal with the charge reading from the ICT. This was done with 30 and 60 ns pulse lengths. The position cavity sensitivity was measured by moving the beam in the pickup using the upstream pair of two-axis dipole corrector magnets. Many position scans were performed at the 2 ns pulse length and these scans could be used to measure the calibration constants across different days. The position sensitivity measurement, however, had to be made using a longer 60 ns pulse length since the charge in the shorter beam pulses was too low to be measured using the ICT. In this section, each data point with error bars is the mean from a sample size of 20 and the typical definition of the standard error is used unless otherwise stated.

A. Control of operational signal range

Adjustment of the cavity BPM signal range to cover different beam pulse lengths and bunch charges is possible using the remotely controlled attenuator in each electronics channel. The performance of the variable attenuator is very important. The nominal values of its attenuation settings must be accurate so that conversions between measurements made using different settings are reliable. If position measurements are to be made at different attenuation settings, no conversion of the calibration constants is necessary as long as the attenuator setting is kept the same in both the position and reference channels and the variation between the two variable attenuators is small. In this case, the change in phase advance with attenuation setting is also important since the phase of the position signal must be known relative to the phase of the reference signal. In a scenario where the attenuation in one channel

TABLE VI. Results of beam based measurements of the variable attenuation in the three BPM channels in comparison with a bench measurement of the variable attenuator.

Channel	Attenuation scan fit gradient
X	-1.0034 ± 0.0016
Y	-0.974 ± 0.002
Bench	-0.9895 ± 0.0009

must be changed while keeping the attenuation in the other channel constant either the calibration constants must be adjusted accordingly or the BPM must be recalibrated. If the calibration constants are to be adjusted, the behavior of the variable attenuator must be known and must be reliable.

The performance of the remotely controlled attenuator was measured using the beam with a 2 ns pulse length. The attenuation setting in each position cavity channel was scanned in steps of 0.5 dB while the attenuation on the reference cavity channel was kept constant. At each attenuation setting, 20 beam pulses were recorded. For each beam pulse, after digital down-conversion to baseband, the output voltage was sampled at the peak and normalized by the output voltage from the reference cavity so that the results are not affected by beam charge variation. A linear fit was then performed in a logarithmic scale. The results are shown in Fig. 7 and are summarized in Table VI. They are compared with bench measurements of the variable attenuator, where the error has been estimated from the standard deviation within a 200 MHz bandwidth of the 15 GHz signal frequency. The resulting gradients of the three fits are not consistent with each other because of

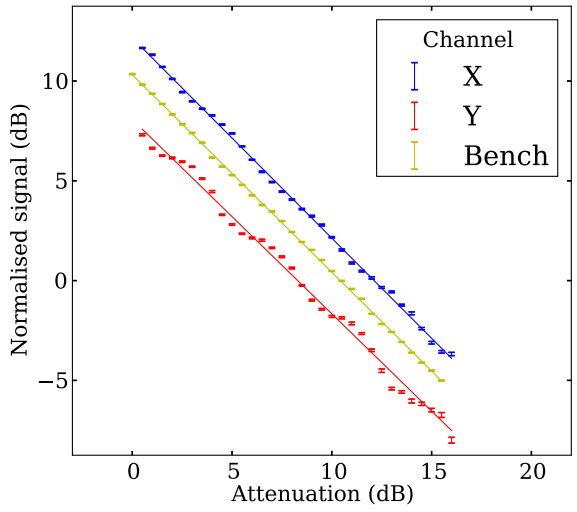

FIG. 7. Peak signals from the horizontal and vertical position cavity channels normalized by the reference cavity signal for the different settings of the digitally controlled variable attenuator. The attenuation in the reference channel was kept constant. Data from the bench measurement of the variable attenuator is included with an artificial offset.

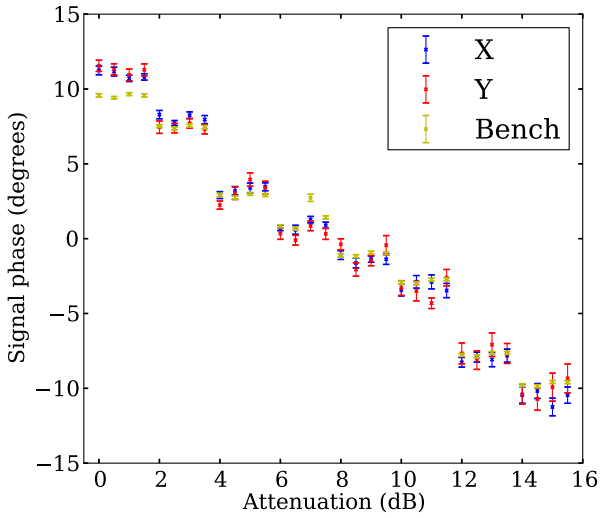

FIG. 8. Phase of the signals from the horizontal and vertical position cavity channels relative to the phase of the reference cavity signal for different settings of the variable attenuator. The attenuation in the reference channel was kept constant. Data from the bench measurement of the variable attenuator is included and all three data sets are mean subtracted.

variation in the attenuator manufacturing. Only the result for the horizontal channel is within 3 standard errors of the ideal value of -1 but they are close enough for the nominal attenuation settings to be used for measurement conversion. There is also a visible systematic uncertainty in the beam based measurements coming from an oscillation of the data points around the linear fit, particularly in the vertical channel. This does not appear in the bench measurement so is almost certainly down to changes in the beam position during the measurement. Based on later calibrations of the cavity BPM (see Sec. III) these position changes would have to have been at the level of about ± 50 μm vertically and correlated in the two transverse directions.

In addition to the change in amplitude, the change in the signal phase relative to the reference signal was measured. This is shown in Fig. 8. The phase advance appears to change in steps of four attenuation settings and varies by over 20°. The same pattern is seen in the variable attenuator bench measurements. Although there are clear differences between certain data points, the results of the three measurements are again similar suggesting that variation in the variable attenuator production is low. This means that the calibration constants will hold as long as the attenuation settings of the reference and position channels are the same. If the setting on one channel is changed and not the other, the change in phase advance is too large to be ignored and the IQ rotation angle would either have to be adjusted or a new beam based calibration would have to be performed.

B. Beam pulse length

In order to test the analytical predictions outlined in Sec. I B, the beam pulse length was scanned by adjusting

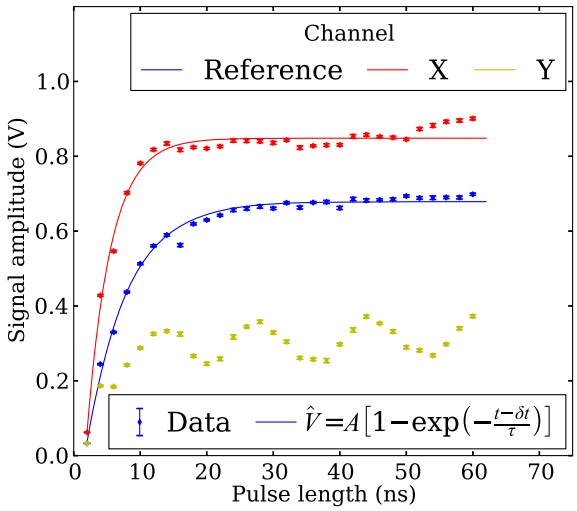

FIG. 9. Maximum reference signal amplitude for different beam pulse lengths.

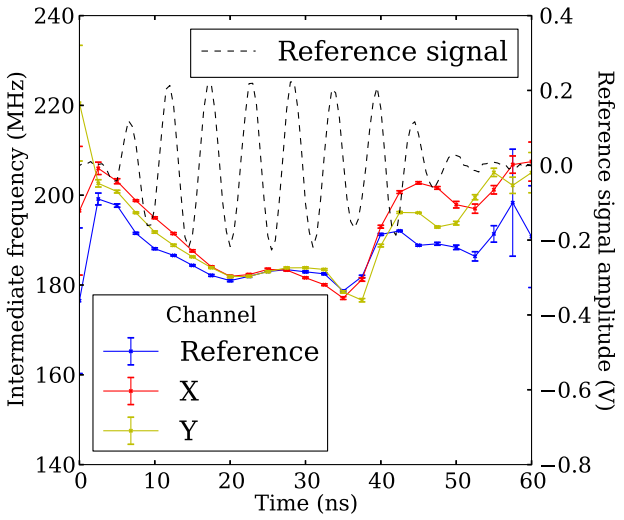

FIG. 10. Signal frequency measured every five samples along the length of 40 ns long pulses.

the timing of the pulse picker for the photoinjector laser. Twenty pulses were recorded for each pulse length and the maximum amplitude of the signal from each channel was measured for each pulse. The results are shown in Fig. 9. There is a clear oscillation of the results in the vertical position channel that also appears to some extent in the horizontal channel. This is due to some periodic beam motion, correlated in the two transverse directions, as seen in the scan of the electronics attenuation in Sec. II A. The vertical channel was therefore excluded from further analysis. A function of the form

$$\hat{V}_{\mathrm{DDC}} = A(1 - e^{-\frac{t-\delta t}{\tau}}) \tag{20}$$

was fitted to the data from the reference and horizontal channels where t is the pulse length requested from the pulse picker and the amplitude limit A, a timing offset δt and the decay time τ are fit parameters. The timing offset parameter is necessary to account for a systematic uncertainty in the actual value for the beam pulse length, which arises from the unknown phase of the laser oscillator at the start of the pulse and timing uncertainties in the pulse picker control. The fits are shown in Fig. 9. For the reference channel, the decay time parameter τ measured using the fit is 5.72 ± 0.14 ns. This value includes the effects of the electronics as well as the resonant cavity mode and so is more than twice the value of 2.8 ns predicted from the quality factor measurement and listed in Table II. Conversely, the measured decay time for the horizontal channel is 3.49 ± 0.08 ns, which is shorter than the value of 4.2 ns predicted from the quality factor measurement. As illustrated in Fig. 1, a small frequency offset from the bunch arrival harmonic reduces the signal rise time and leads to a shorter result for the decay time measurement. The covariance between the frequency offset and the decay time is too large to include both as fit parameters. Equation (12) also assumes that each bunch arrives with the same position offset. Changes in position during the start of the bunch train or between data points could heavily influence the measurement. The digitized signal in Fig. 6 from the long beam pulse shows clear amplitude variation due to changes in position between bunches.

The signal frequency, determined as the frequency of the digital LO that minimizes the change in the phase of the baseband signal over time (as in [4]), was also measured along the length of 20 pulses, each 40 ns long. Five digitizer samples were used for each of the frequency measurements and the variation between pulses was used to estimate the statistical uncertainty. The results are shown in Fig. 10. The variation in the frequency throughout the pulse is partly due to the response of the electronics, which is affected by reflections and nonlinearities. The dominant source of differences between the behavior of the three channels, on the other hand, is the looser manufacturing tolerances of the more narrow band cavity pickup. As a consequence of the convergence of Eq. (6), the signal becomes periodic at the bunching frequency when the signal reaches steady state amplitude. The frequencies of the three signals can therefore be seen to converge. Phase changes due to position variation in the tail of the bunch train manifest themselves as small changes in frequency. Then, during the decay of the signal, where the frequency is defined by the geometry of the pickup as no bunches are passing, the results for the three channels are again significantly different. The largest difference seen, of around 10 MHz, is small enough to be attributed to the manufacturing tolerances. Indeed, in the bench measurements, the results of which are listed in Table II, a difference of 15 MHz was observed between the reference cavity and one of the position channels. The largest frequency change in one channel

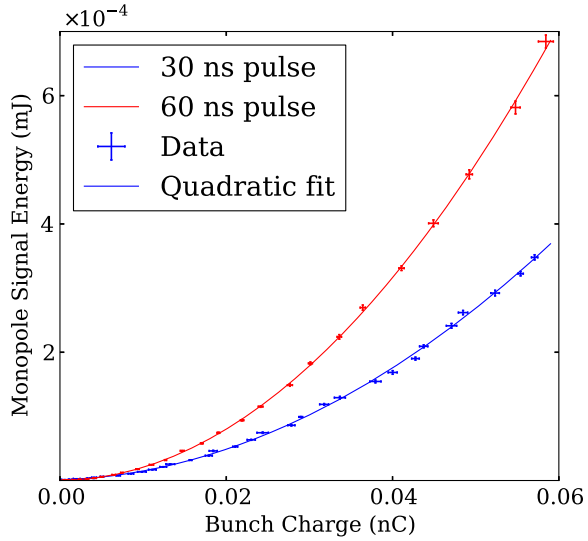

FIG. 11. Total signal energy from the reference cavity for different bunch charges and pulse lengths of 30 and 60 ns.

was about 25 MHz. This is larger than the 12 MHz detuning from 15 GHz seen in the bench measurements but an uncertainty in the frequency of the 3 GHz rf system could account for the difference, especially since any error would be multiplied at the fifth harmonic. A 25 MHz frequency offset would also account for the short decay time measured for the horizontal position channel using the fit in Fig. 9. Oscillation at the signal mode resonant frequency that occurs between bunches is not distinguishable because the bandwidth of the electronics is much smaller than the 1.5 GHz bunch arrival frequency.

C. Charge sensitivity

The sensitivity of the reference cavity signal to charge was measured by varying the power of the photoinjector laser on the cathode. The total beam pulse charge was measured using the ICT and the bunch charge was determined by dividing the pulse charge by the number of bunches expected for the pulse length. The measured signal energy was determined for 20 pulses at each pulse charge setting using Eq. (19). Figure 11 shows the measured signal energy against the bunch charge. The results are for two different pulse lengths on two different days, 30 ns corresponding to about 45 bunches and 60 ns corresponding to 90 bunches. A quadratic fit is used to determine the signal sensitivity and the results of the fits are in Table VII where the single bunch result has been estimated using Eq. (14). The result for the 30 ns pulse length, 0.099 ± 0.007 mJ nC^{-2}, and the result for the 60 ns pulse length, 0.196 ± 0.009 mJ nC^{-2}, are both consistent with their respective predicted values of 0.0932 and 0.196 mJ nC^{-2}. The results convert to single bunch sensitivity values of 145 ± 5 and 141 ± 3 V nC^{-1} respectively, which correspond well to the prediction of 141 V nC^{-1}.

D. Position sensitivity

The position sensitivity was measured in the horizontal direction by using the upstream two-axis dipole corrector magnets to change the position of the beam in the cavity BPM pickup. For these measurements, the final quadrupole triplet shown in Fig. 4 was switched off so that a simple ballistic model for the beam trajectory could be used. The angular response of the beam to each corrector was measured beforehand using the profile monitor YAG screen that is downstream of the correctors and upstream of the pickup. Based on the measured response, the value used to predict the change in beam position at the cavity BPM pickup due to a change in corrector current is -0.64 mm m^{-1} A^{-1} for a 208 MeV beam. As well as using the downstream corrector alone, the two correctors were used antagonistically as a pair so that, assuming the same angular response for both correctors, the beam offset could be adjusted without changing the beam trajectory angle. The position response in this case was measured to be 1.30 mm A^{-1}.

The beam position in the cavity BPM pickup was varied in steps and at each position step, the signals from 20 beam pulses, each 60 ns long, were recorded and the energy in each signal was calculated. The energy was then normalized by the square of the pulse charge to remove the effects of the pulse to pulse charge variation. Fourteen scans were made, seven using a single corrector and seven using both correctors. A quadratic fit was performed to the results of each scan, an example of which is shown in Fig. 12. The averaged results are shown in Table VII where the single bunch response has been calculated.

TABLE VII. Results of measurements of the reference cavity sensitivity to bunch charge and the position cavity to a change in horizontal beam position with the corresponding single bunch sensitivities calculated using Eq. (14).

Sensitivity	Channel gain (dB)	Total energy (mJ nC^{-2})		Single bunch peak voltage (V nC^{-1})	
		Predicted	Measured	Predicted	Measured
Reference (30 ns pulse)	−17.7	0.0932	0.099 ± 0.007	141	145 ± 5
Reference (60 ns pulse)		0.196	0.196 ± 0.009		141 ± 3
Position (single corrector)	−6.0	9.41×10^{-3} mm^{-2}	$(9.85 \pm 0.09) \times 10^{-3}$ mm^{-2}	20.6 mm^{-1}	21.05 ± 0.10 mm^{-1}
Position (corrector pair)			$(9.72 \pm 0.09) \times 10^{-3}$ mm^{-2}		20.91 ± 0.10 mm^{-1}

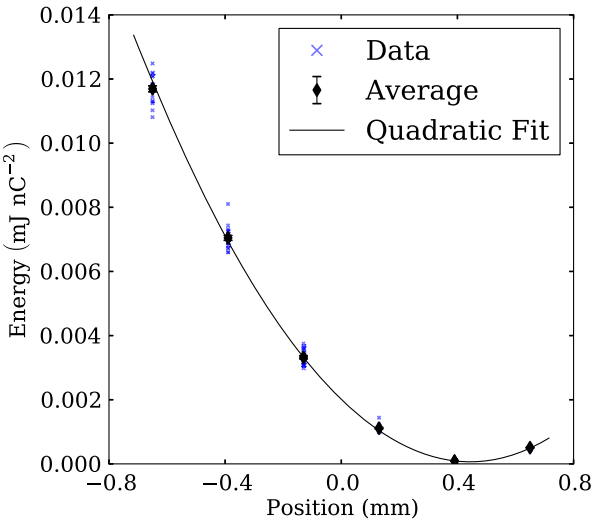

FIG. 12. Total signal energy from the horizontal position cavity channel normalized by bunch charge squared during a sweep in the horizontal beam position.

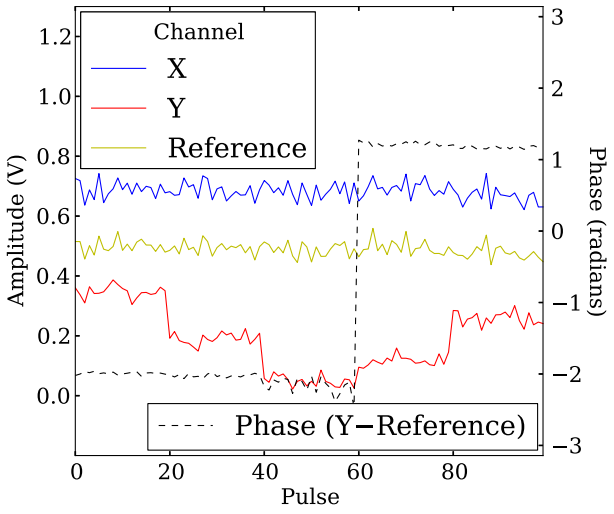

FIG. 13. Signal amplitudes from the different channels during a vertical calibration with the phase of the signal from the vertical position cavity channel also shown.

For the charge normalization, the reference cavity had to be used because the ICT is not able to provide pulse to pulse measurements. The average pulse charge measured by the reference cavity over the 14 position scans was -3.486 ± 0.011 nC and this can be compared to the average charge of -3.57 ± 0.009 nC measured using the ICT. The two results for the average charge differ by 3%, which is a small systematic uncertainty.

The average results for the two sets of measurements, those made using a single corrector and those made with the corrector pair, are $(9.85 \pm 0.09) \times 10^{-3}$ and $(9.72 \pm 0.09) \times 10^{-3}$ mJ nC^{-2} mm^{-2} respectively. They differ by approximately the combined standard error and so are consistent and are both within 5% of the predicted value of 9.41×10^{-3} mJ nC^{-2} mm^{-2}. They convert to single bunch sensitivity results of 21.05 ± 0.10 and 20.91 ± 0.10 V nC^{-1} mm^{-1} respectively, in comparison with the prediction of 20.6 V nC^{-1} mm^{-1}.

III. CALIBRATION AND POSITION JITTER

Calibrations were performed in order to determine the two calibration constants required for position measurements. These are the IQ rotation angle θ_{IQ} and the position scale factor s introduced in Sec. I D. One or two dipole corrector magnets were used to change the position of the beam in the pickup in steps and at each step, the signals from 20 short 2 ns beam pulses were recorded. Digital down-conversion was then used to convert the digitized signals to baseband. The start time of the signal from each pulse was measured from the rising edge of the diode-rectified output of the reference cavity and the timing offsets between the different channels were measured beforehand. The amplitude and phase of the down-converted signals were then sampled 15 ns after the signal rise.

Figure 13 shows the signal amplitude for the three channels during a calibration in the vertical direction along with the phase in the vertical position (Y) channel relative to the reference phase. The position steps are clearly visible in the Y channel while the other two channels are roughly constant in amplitude. There is also a step change in the phase of the vertical signal when the beam crosses the center of the cavity pickup. When the beam is close to the center of the cavity, this phase change is not exactly π because there is a small residual signal due to the beam trajectory angle and bunch tilt and pollution from the position cavity monopole modes which strongly couple to the beam. As the beam offset increases however, the phase change does approach π as these contributions become negligible.

After the three channels have been measured individually, the position signals are normalized by the reference signal amplitude and the difference in phase between the position and reference cavity signals is determined. Equation (17) is then used to determine the in-phase I and quadrature-phase Q components for each beam pulse and each transverse direction. Figure 14 shows a plot of Q against I for vertical signals during a position scan in the vertical direction. It is assumed that the step changes in I and Q are the result of changes in beam position only. A linear fit is performed to the data to determine the IQ rotation angle, which is the arctangent of the fit gradient. The rotation by this angle is then applied so that the step changes appear in one component only. The result is shown in Fig. 15 where the two resulting signals, the "Position" signal and the "Tilt" signal, have been plotted against the predicted beam position as determined from the measured angular response of the dipole corrector magnets. A second linear fit has been applied to determine the position scale factor to convert the position signal to physical units, in this case millimeters.

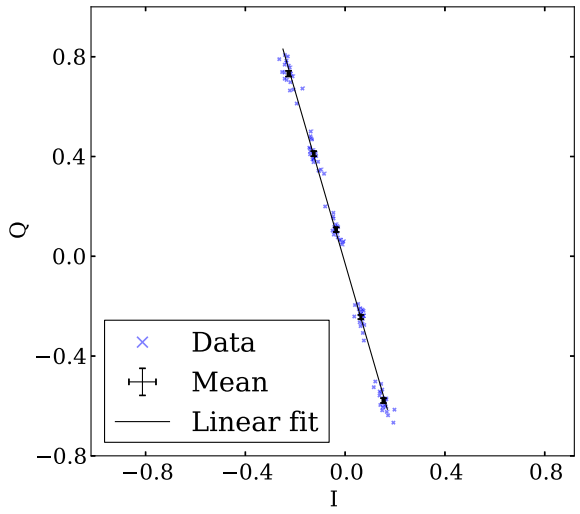

FIG. 14. Fit of the quadrature-phase component of the vertical position cavity signal against the in-phase component during a vertical position scan to measure the IQ rotation angle.

Calibrations were also performed in the horizontal direction. On the 13th of May, 2013, the average IQ rotation angles measured were $71.51 \pm 0.10°$ in the horizontal direction and $-84.31 \pm 0.12°$ in the vertical direction (standard errors). The average scale factors were measured to be -0.886 ± 0.003 and -0.923 ± 0.015 mm in the horizontal and vertical directions respectively. The position scale factors in the two transverse directions are within 3 standard errors of each other, which confirms that the cavity BPM is equally sensitive to vertical beam offsets as to horizontal beam offsets.

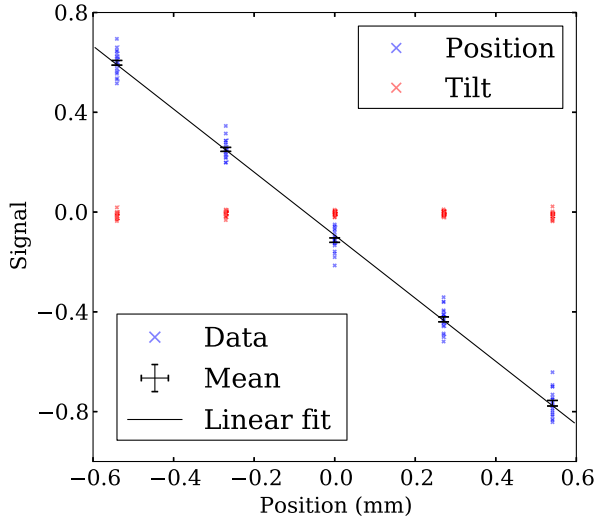

FIG. 15. Fit of vertical position signal amplitude against the predicted beam position to measure the position scale factor. The tilt signal from the bunch tilt and beam trajectory angle is also shown.

The position scale factor s can be predicted as

$$s = \frac{G_r S_r}{G_p S_p}, \tag{21}$$

where G is the total channel gain, S is the pickup output sensitivity and the subscripts r and p again denote the position and reference cavity signals respectively. The prediction from the measured single bunch sensitivities for the 60 ns pulse length and the channel gains in Table VII is 1.75 mm. This is much larger than the measured values because of the wide bandwidth of the reference cavity monopole mode compared to the position cavity dipole mode. From the difference in reference and position signal decay during the signal rise time of 5 ns, crudely estimated from inspection of Fig. 6, a naive estimate for the expected difference is a factor of 1.8, almost the difference seen.

Once a beam based calibration had been carried out, the pulse to pulse beam position jitter at the location of the BPM pickup was measured for the same 2 ns pulse length. This was done with the final quadrupole triplet in Fig. 4 switched off and then switched on to focus the beam at the location of the pickup and reduce the position jitter, which is expected to be a constant fraction of the beam size. No dedicated data was taken for the jitter measurement so for each transverse direction, 100 pulses were taken from a position scan in the perpendicular direction. The standard deviation in beam position over the 100 pulses was calculated; the results are listed in Table VIII. The scale factor in all three cases was taken from calibrations on the 13th of May while the IQ rotation angle, which has a dependence on the signal frequency and the channel timing offsets as discussed in [4], was measured separately on each day. It is clear that the position jitter decreases with the predicted beam size when the quadrupole triplet is switched on. The minimum position jitter measured was 13 μm, which is about 20% of the predicted beam size at that time. In all other cases, the measured position jitter is about 10% of the beam size.

The digitizer was measured to have an effective resolution of 8.4 bits [9]. For the pulse charge of 0.05 nC that was measured on the 6th May using the reference cavity, a position cavity sensitivity of 21 $\mathrm{V\,nC^{-1}\,mm^{-1}}$ and the measured -6 dB gain of the analogue processing and signal transfer cables, this leads to a rough estimate of

TABLE VIII. Results of beam position jitter measurements on different days along with the predicted beam size at the time of two of the results [23].

Date 2013	Final triplet used	Position jitter (μm)		Beam size (μm)	
		X	Y	X	Y
6th May	No	20	34	190	390
6th May	Yes	13	27	60	260
13th May	No	18	78	...	...

11.3 μm for the position resolution. Combined in quadrature with the 6 μm of beam jitter expected for the predicted beam size, this gives 12.8 μm for the position jitter that would be observed. This is very close to the measured value of 13 μm so it is reasonable to conclude that the position jitter measurement is limited by the BPM resolution. Upgrading to a digitizer with 12 effective bits, removing some of the fixed attenuation and adding 14 dB of gain to the electronics should allow the targeted resolution of 50 nm to be achieved with a single bunch of 0.1 nC charge.

IV. CONCLUSION

A prototype cavity BPM pickup for the Compact Linear Collider was manufactured and has been tested on the probe beam line of CTF3 at CERN. Analytical expressions for the signal amplitude and phase when the pickup is excited by long trains of closely spaced bunches have been derived. It is found that the signal converges in amplitude and phase at the arrival time of each bunch and therefore becomes periodic with the bunching frequency. As a result of the convergence, the measured signal frequency of all three channels becomes dominated by the harmonic of the bunching frequency that is closest to the cavity resonant frequency.

A set of receiver electronics with three channels was installed close to the BPM pickup and measured using the beam excited signals. The sensitivity of the pickup was determined from the total signal energy extracted from the two pickup cavities and was compared with theoretical predictions based on the R/Q s and quality factors of the modes of interest. The sensitivity of the reference cavity signal to bunch charge was measured for two pulse lengths, 30 ns and 60 ns. The results for the single bunch sensitivity, 145 ± 5 and $141 \pm 3 \mathrm{VnC}^{-1}$ respectively, are both consistent with the predicted value of 141 $\mathrm{V\,nC^{-1}}$. The sensitivity of the horizontal position signal to beam offset was also measured using a single corrector or a corrector pair. The respective results of $(9.85 \pm 0.09) \times 10^{-3}$ and $(9.72 \pm 0.09) \times 10^{-3}$ $\mathrm{mJ\,nC^{-2}\,mm^{-2}}$ are both less than 5% larger than the prediction of 9.41×10^{-3} $\mathrm{mJ\,nC^{-2}\,mm^{-2}}$. The results convert to single bunch voltage sensitivities of 21.05 ± 0.10 and 20.91 ± 0.10 $\mathrm{V\,nC^{-1}\,mm^{-1}}$ respectively. both of which are about 2% larger than the predicted value of 20.6 $\mathrm{V\,nC^{-1}\,mm^{-1}}$. There is, therefore, good agreement between the measured pickup sensitivity and the theoretical predictions.

The BPM was calibrated to determine the IQ rotation angle and position scale factor so that the beam position could be measured in physical units. The beam position jitter at the location of the BPM was then measured and compared with the beam size. The minimum value for the measured position jitter, 13 μm, is larger than the other measured values as a fraction of the predicted beam size and so could be affected by the BPM position resolution. It is close to the predicted measurement result of 12.8 μm, based on the estimated resolution of the current setup and taking 10% of the predicted beam size as the position jitter. A second generation of the pickup has been designed [19] and if the design is successful, at least three will be manufactured in order to be able to subtract the beam position jitter and make a dedicated measurement of the position resolution. This will also allow the measurement bandwidth of the BPM to be determined.

ACKNOWLEDGMENTS

The mechanical design of the beam line installation is the work of David Bastard at CERN and the construction of the electrical installations is that of Phillippe Lavanchy and Laurent Payraud. The control board for the remotely controlled attenuators was designed and programed by Gary Boorman at Royal Holloway and constructed by Ola Popoola. Many thanks are owed to the technical support staff at CERN who worked to ensure that the full installation was complete before the start of beam operation. We would like to acknowledge CERN for financial support of this research within CLIC-UK collaboration: Contract No. KE1870/DG/CLIC. This research has received funding from the Science and Technologies Facilities Council. The computing time with ACE3P was provided by U.S. DOE at NERSC.

[1] M. Aicheler *et al.*, A multi-TeV linear collider based on CLIC technology: CLIC conceptual design report, Technical Report No. CERN-2012-007, CERN, Geneva, 2012.

[2] A. Latina, J. Pfingstner, D. Schulte, and E. Adli, Performance of linear collider beam-based alignment algorithms at FACET, in *Proceedings of the 3rd International Particle Accelerator Conference, New Orleans, LA, 2012* (IEEE, Piscataway, NJ, 2012), p. TUPPR029.

[3] D. Schulte, Different options for dispersion free steering in the CLIC main linac, in *Proceedings of the 21st Particle Accelerator Conference, Knoxville, TN, 2005* (IEEE, Piscataway, NJ, 2005), p. RPPP011.

[4] Y. I. Kim *et al.*, Cavity beam position monitor system for the accelerator test facility 2, Phys. Rev. ST Accel. Beams **15**, 042801 (2012).

[5] D. M. Pozar, *Microwave Engineering*, 3rd ed. (Wiley, New Jersey, 2005), pp. 6,124,284.

[6] S. Walston *et al.*, Performance of a high resolution cavity beam position monitor system, Nucl. Instrum. Methods Phys. Res., Sect. A **578**, 1 (2007).

[7] D. H. Whittum and Y. Kolomensky, Analysis of an asymmetric resonant cavity as a beam monitor, Rev. Sci. Instrum. **70**, 2300 (1999).

[8] N. Chritin *et al.*, A high-resolution cavity BPM for the CLIC test facility, in *Proceedings of the 14th Beam Instrumentation Workshop, Santa Fe, NM* (LANL, Los Alamos, 2010), p. TUPSM32.

[9] F. J. Cullinan, Development of a prototype cavity beam position monitor for the compact linear collider, Ph.D. thesis, Royal Holloway, University of London, 2014.

[10] K. Ko *et al.*, Advances in parallel electromagnetic codes for accelerator science and development, in *Proceedings of the 25th International Linear Accelerator Conference, LINAC-2010, Tsukuba, Japan* (KEK, Tsukuba, Japan, 2010), p. FR101.

[11] W. Bruns, GdfidL: A finite difference program with reduced memory and CPU usage, in *Proceedings of the Particle Accelerator Conference, Vancouver, BC, Canada, 1997* (IEEE, New York, 1997), p. 9P118.

[12] C. Hessler *et al.*, Recent developments at the high-charge PHIN photoinjector and the CERN photoemission laboratory, in *Proceedings of the 5th International Particle Accelerator Conference, Dresden, 2014* (EPS-AG, Mulhouse, 2014), p. MOPRI042.

[13] M. Wendth *et al.*, Status of the CLIC/CTF beam instrumentation R&D, in *Proceedings of the 5th International Particle Accelerator Conference, Dresden, 2014* (EPS-AG, Mulhouse, 2014), p. THPME178.

[14] R. Ruber, V. Ziemann, T. Ekelöf, A. Palaia, W. Farabolini, and R. Corsini, The CTF3 Two-beam test stand, Nucl. Instrum. Methods Phys. Res., Sect. A **729**, 546 (2013).

[15] C. Simon *et al.*, Beam position monitors using a reentrant cavity, in *Proceedings of the 8th European Workshop on Beam Diagnostics and Instrumentation for Particle Accelerators, Venice, 2007* (Elettra, Trieste, 2007), p. TUPB15.

[16] M. Gasior, An inductive pickup for beam position and current measurements, in *Proceedings of the 6th European Workshop on Beam Diagnostics and Instrumentation for Particle Accelerators, Mainz, 2003* (GSI, Darmstadt, 2003), p. CT01.

[17] W. Farabolini *et al.*, Video profile monitor development for the CTF3 probe beam linac, in *Proceedings of the 11th European Particle Accelerator Conference, Genoa, 2008* (EPS-AG, Genoa, Italy, 2008), p. TUPC024.

[18] Hittite Microwave Corporation, http://www.hittite.com/, 2012.

[19] J. R. Towler *et al.*, Technologies and R&D for a high resolution cavity BPM for the CLIC main beam, in *Proceedings of the 2nd International Beam Instrumentation Conference, Oxford, 2013* (Diamond Light Source, Oxford, 2013), p. TUPC20.

[20] Agilent Technologies, http://www.home.agilent.com/en/pd-1184897-pn-U1065A/acqiris-10-bit-high-speed-cpci-digitizers, 2012.

[21] Oasis, https://project-oasis.web.cern.ch/project-oasis/, 2013.

[22] M. Arruat *et al.*, Front-end software architecture, in *Proceedings of the International Conference on Accelerator and Large Experimental Physics Control Systems, Knoxville, 2007* (IEEE, Piscataway, NJ, 2007), p. WOPA04.

[23] W. Farabolini (personal communication).